Supporting Information

Promoting and Tuning Porosity of Flexible Ether-Linked Phthalazinone-Based Covalent Triazine Frameworks Utilizing Substitution Effect for Effective CO_2 Capture

Kuanyu Yuan,[a] Cheng Liu,*[a] Lishuai Zong,[a] Guipeng Yu,[b] Shengli Cheng,[a] Jinyan Wang,[a] Zhihuan Weng [a] and Xigao Jian*[a]

[a] State Key Laboratory of Fine Chemicals, Dalian University of Technology, Dalian, 116024, China. E-mail: jian4616@dlut.edu.cn.

Department of Polymer Science and Materials, Dalian University of Technology, Dalian, 116024, China. E-mail: liuch1115@dlut.edu.cn

Liaoning Province Engineering Research Centre of High Performance Resins, Dalian, 116024, China.

[b] College of Chemistry and Chemical Engineering, Central South University, Changsha, 410083, China.

Calculation methods:

1) Calculation methods for isosteric heat of adsorption

The isosteric enthalpies (Q_{st}) of CO_2 in PHCTFs were calculated from the adsorption isotherms measured at differernt temperatures in term of Clausius-Clapeyron equation:

$$\ln P = \frac{Q_{st}}{RT} + C \quad (1)$$

where R, C, P and T are the gas constant, equation constant, the pressure and temperature at the equilibrium state, respectively.

2) Calculation methods for Q_0, A_0, K_H values

The first virial coefficients (A_0) are obtained from the slopes of the virial plots. From their intercepts, A_0 values relating to gas-material interaction were calculated. Henry's law constants (K_H) are calculated from the equation K_H = exp (A_0). Then, the limiting enthalpy of adsorption at zero surface CO_2 coverage (Q_0) can be obtained in term of Vant Hoff equation:

$$\frac{d\,[\ln K_H]}{dT} = \frac{Q_0}{RT^2} \quad (2)$$

3) Calculations for Selectivities of CO_2/CH_4 and CO_2/N_2 gas pairs by IAST method

Ideal adsorbed solution theory (IAST) was performed to evaluate the adsorption selectivities of CO_2/CH_4 and CO_2/N_2 gas mixtures. According to Myers and Prausnitz, the method of IAST can be reduced to the mathematical integration:

$$\int_{t=0}^{\frac{Py_1}{X_1}} F_1(t)d\ \ln t = \int_{t=0}^{\frac{Py_2}{X_2}} F_2(t)d\ \ln t \quad (3)$$

where P is the total pressure, x_i is the adsorbed phase molar ratio of gas i, y_i is the bulk phase molar ratio of gas i and the function F_i (t) is a fitting function for the pure component i based on the single-site Langmuir-Freundlich model:

$$n = \frac{a \cdot b \cdot p^{1/c}}{1 + b \cdot p^{1/c}} \quad (4)$$

Where n is amount of gas adsorbed (mmol g^{-1}), p is the pressure (bar) of the bulk gas at equilibrium with the adsorbed phase, a is the saturation capacity (mmol g^{-1}), b is the single-site affinity coefficient (1/bar), c is the deviation from an ideal homogeneous surface. These isothermal parameters (a, b, c) are the fitting parameters according to the experimental pure-component isotherms of N_2, CO_2 and CH_4.

Since $x_1 + x_2 = 1$ and $y_1 + y_2 = 1$, the adsorption selectivity ($\alpha_{A/B}$) of gas A over gas B is defined as:

$$\alpha_{A/B} = \frac{x_A/y_A}{x_B/y_B} \quad (5)$$

Supplementary Figures and Tables:

Figure S1. ^{1}H NMR spectrum of DHPZ-DN.

Figure S2. ^{13}C NMR spectrum of DHPZ-DN.

Figure S3. ^{1}H NMR spectrum of MDHPZ-DN.

Figure S4. ^{13}C NMR spectrum of MDHPZ-DN.

Figure S5. ^{1}H NMR spectrum of DMDHPZ-DN.

Figure S6. ^{13}C NMR spectrum of DMDHPZ-DN.

Figure S7. ^{1}H NMR spectrum of PDHPZ-DN.

Figure S8. ^{13}C NMR spectrum of PDHPZ-DN.

Figure S9. ^{1}H NMR spectrum of DPDHPZ-DN.

Figure S10. ^{13}C NMR spectrum of DPDHPZ-DN.

Figure S11. FT-IR spectra of the building blocks.

Figure S12. Thermogravimetric analysis (TGA) data for PHCTFs.

Figure S13. Field-emission scanning electron micrographs (FE-SEM) images (Left) and transmission electron microscopy (TEM) images (Right) of PHCTF-4.

Figure S14. Field-emission scanning electron micrographs (FE-SEM) images (Left) and transmission electron microscopy (TEM) images (Right) of PHCTF-5.

Figure S15. Field-emission scanning electron micrographs (FE-SEM) images (Left) and transmission electron microscopy (TEM) images (Right) of PHCTF-6.

Figure S16. Field-emission scanning electron micrographs (FE-SEM) images (Left) and transmission electron microscopy (TEM) images (Right) of PHCTF-7.

Figure S17. Adsorption selectivity of CO_2 over CH_4 and N_2 for PHCTFs calculated from Henry's law initial slope method at 273 K.

Figure S18. Experimental pure component isotherms for CO_2, CH_4 and

N_2 at 273 K and their corresponding single-site Langmuir-Freundlich curves (solid orange lines).

Table S1. Elemental analysis for PHCTFs polymer networks and ICP results

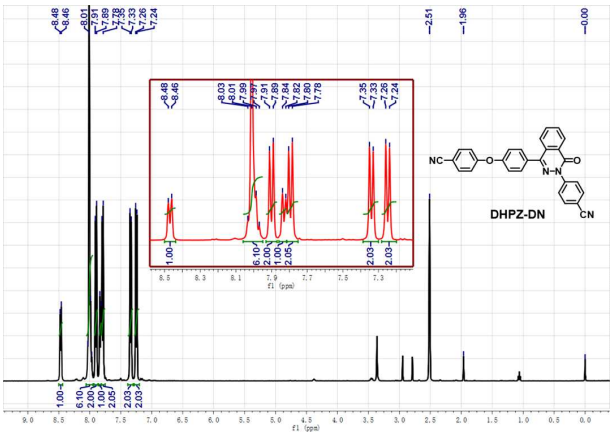

Figure S1. ^{1}H NMR spectrum of DHPZ-DN.

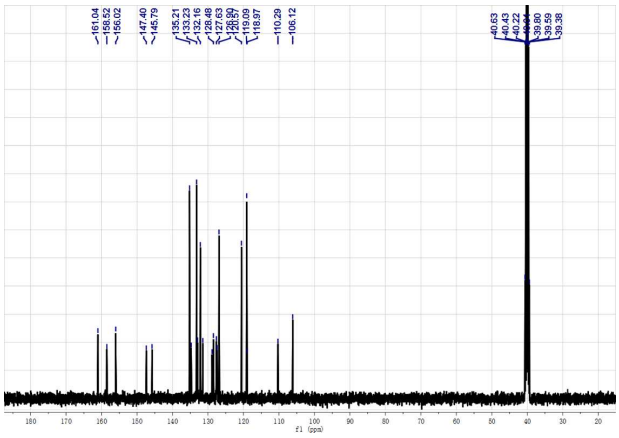

Figure S2. ^{13}C NMR spectrum of DHPZ-DN.

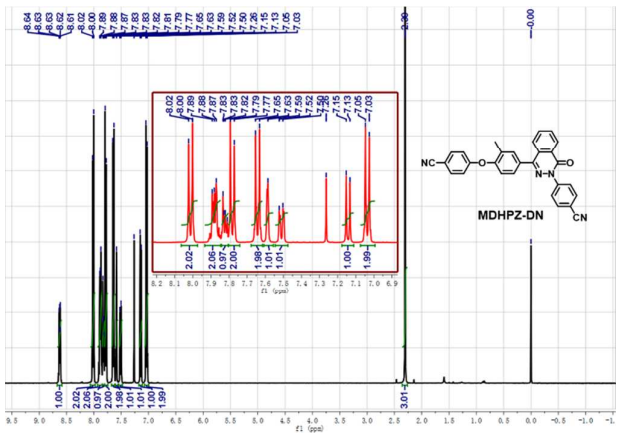

Figure S3. ^{1}H NMR spectrum of MDHPZ-DN.

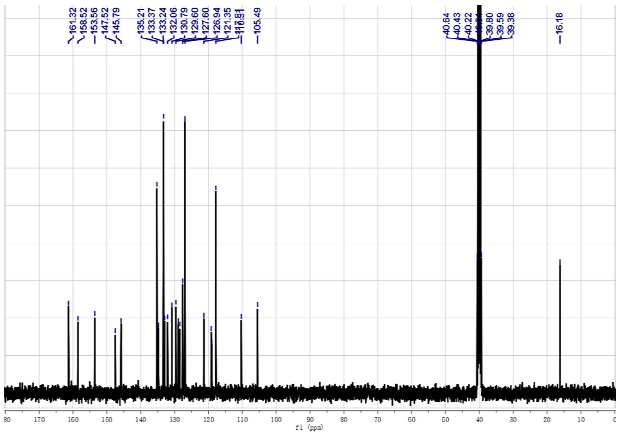

Figure S4. ^{13}C NMR spectrum of MDHPZ-DN.

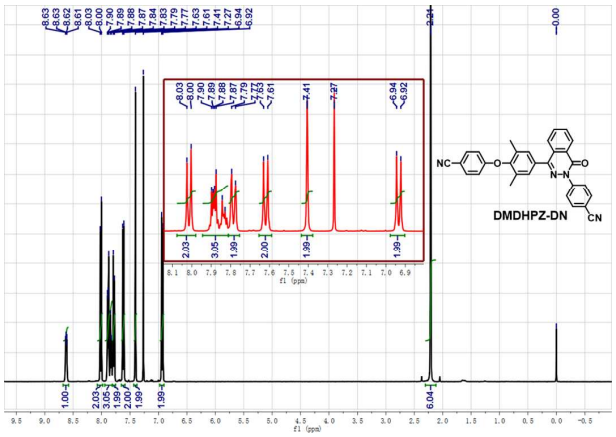

Figure S5. ^{1}H NMR spectrum of DMDHPZ-DN.

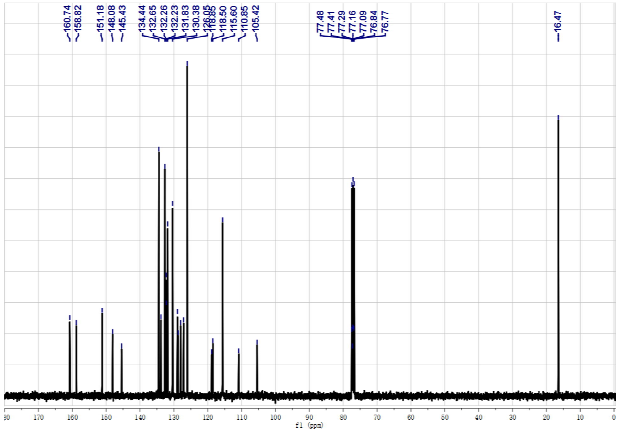

Figure S6. ^{13}C NMR spectrum of DMDHPZ-DN.

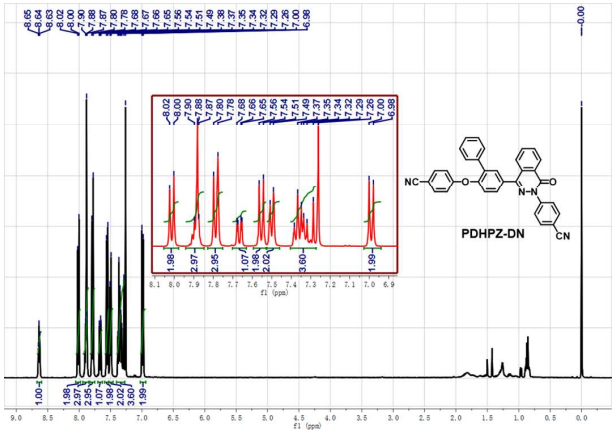

Figure S7. ^{1}H NMR spectrum of PDHPZ-DN.

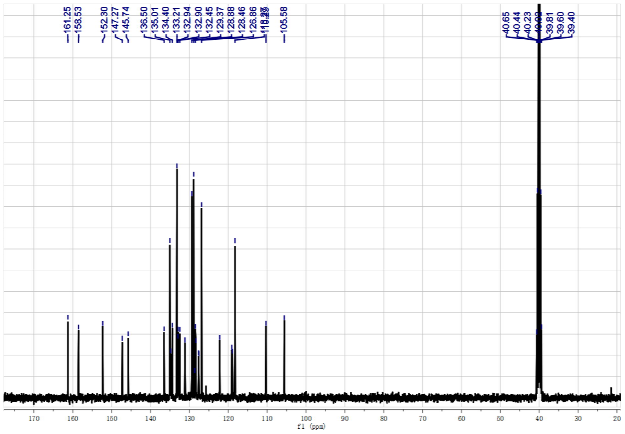

Figure S8. ^{13}C NMR spectrum of PDHPZ-DN.

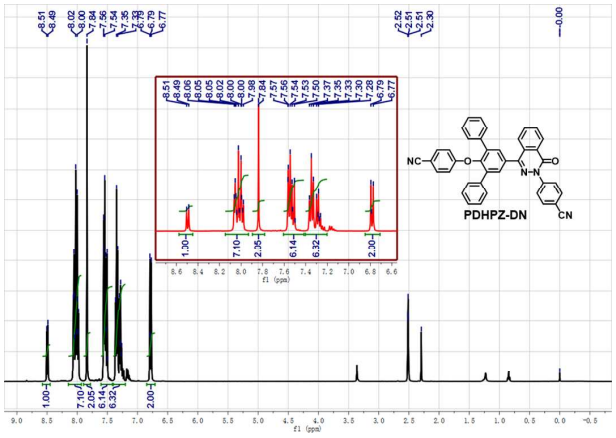

Figure S9. ^{1}H NMR spectrum of DPDHPZ-DN.

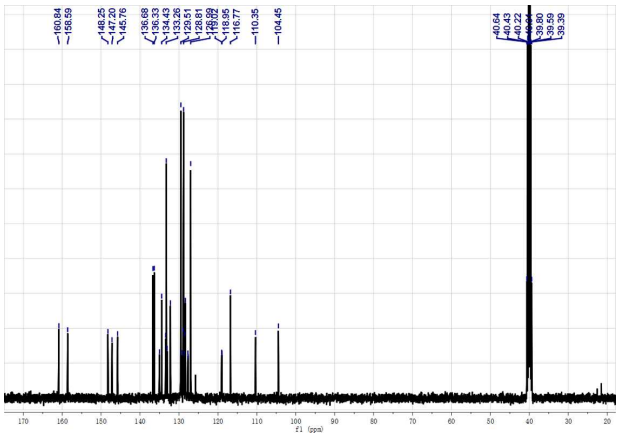

Figure S10. ^{13}C NMR spectrum of DPDHPZ-DN.

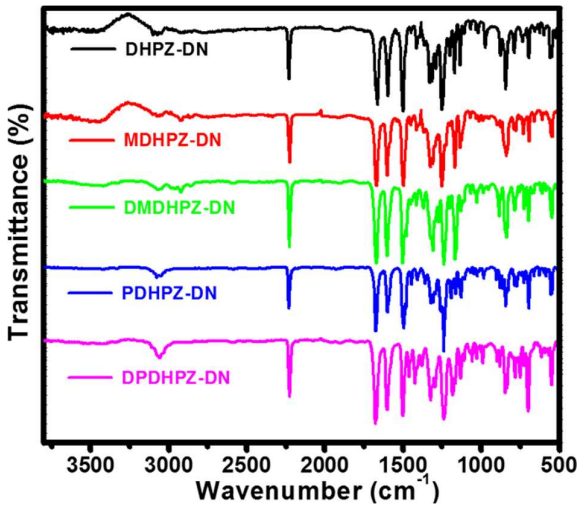

Figure S11. FT-IR spectra of the building blocks.

Table S1. Elemental analysis for PHCTFs polymer networks and ICP results.

samples	Expected C %	Expected H %	Expected N %	Found C %	Found H %	Found N %	ICP(Zn) wt %
PHCTF-3	76.35	3.66	12.72	74.89	3.56	5.90	0.061
PHCTF-4	76.64	3.99	12.33	73.41	4.04	5.07	0.042
PHCTF-5	76.91	4.30	11.96	74.67	3.28	4.09	0.044
PHCTF-6	79.06	3.90	10.85	74.94	3.14	4.51	0.064
PHCTF-7	81.07	4.08	9.45	77.57	3.76	3.56	0.053

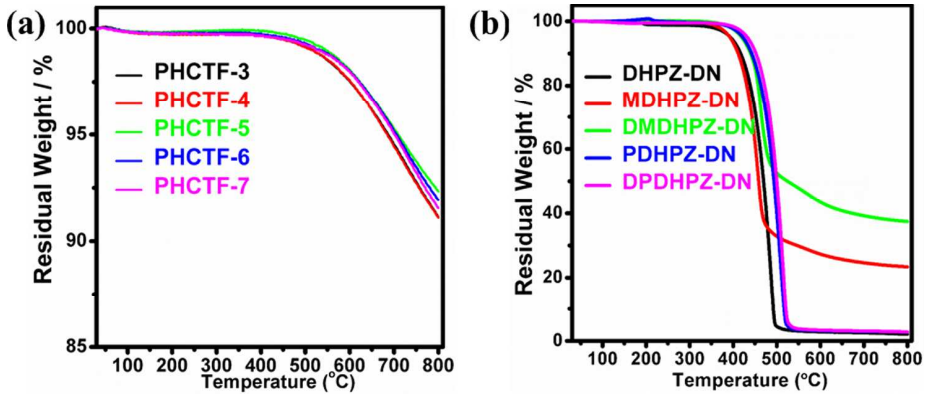

Figure S12. Thermogravimetric analysis (TGA) data for PHCTFs (a) and the building blocks (b)

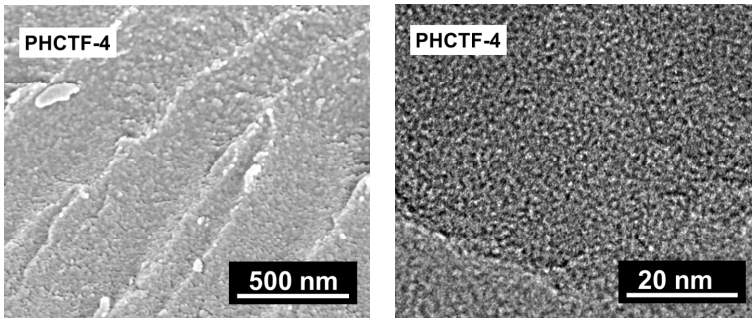

Figure S13. Field-emission scanning electron micrographs (FE-SEM) images (Left) and transmission electron microscopy (TEM) images (Right) of PHCTF-4.

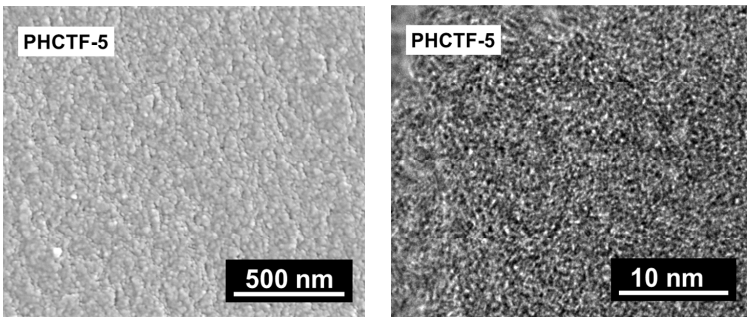

Figure S14. Field-emission scanning electron micrographs (FE-SEM) images (Left) and transmission electron microscopy (TEM) images (Right) of PHCTF-5.

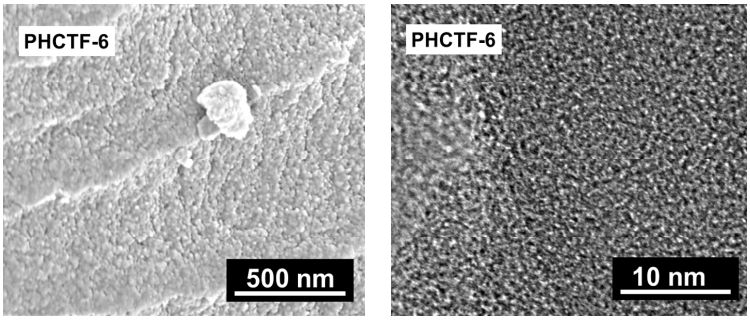

Figure S15. Field-emission scanning electron micrographs (FE-SEM) images (Left) and transmission electron microscopy (TEM) images (Right) of PHCTF-6.

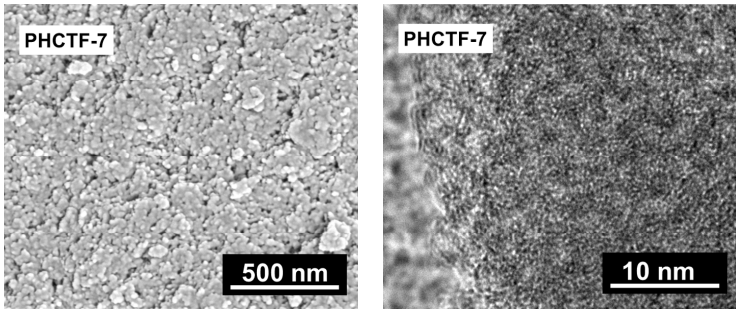

Figure S16. Field-emission scanning electron micrographs (FE-SEM) images (Left) and transmission electron microscopy (TEM) images (Right) of PHCTF-7.

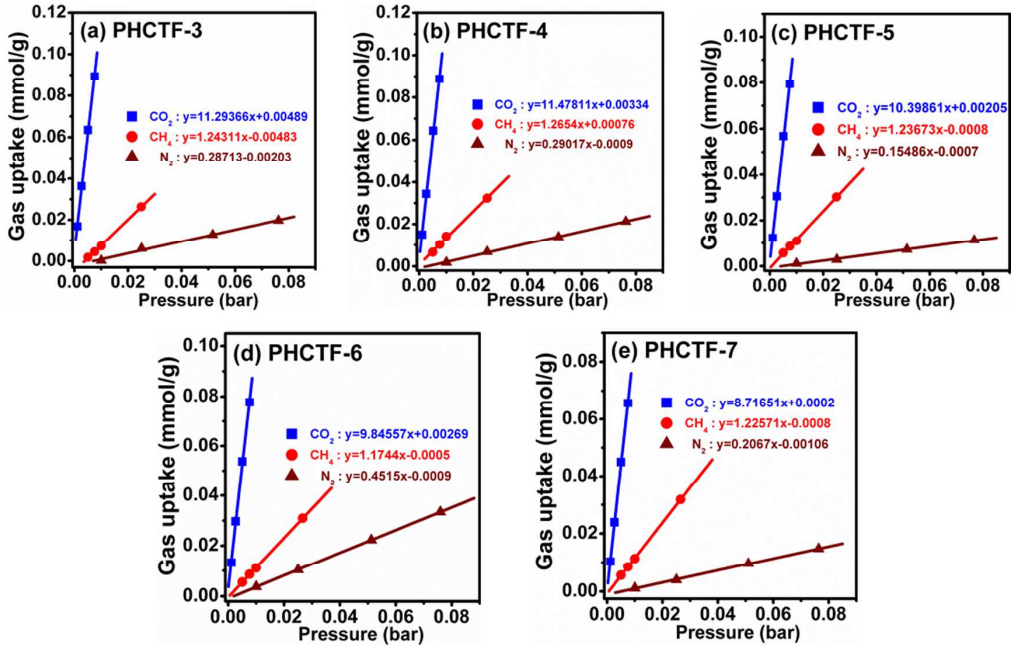

Figure S17. Adsorption selectivity of CO_2 over CH_4 and N_2 for PHCTFs calculated from Henry's law initial slope method at 273 K.

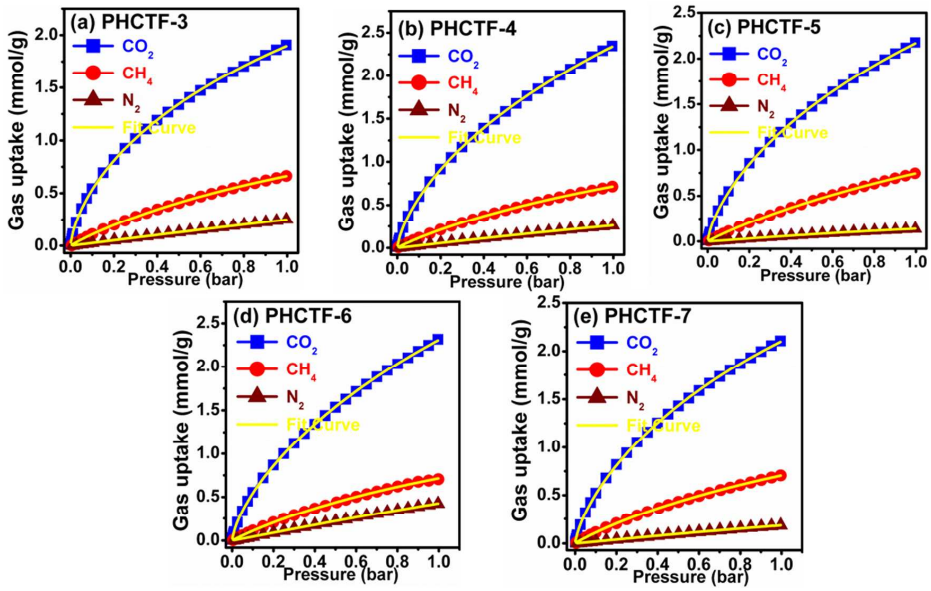

Figure S18. Experimental pure component isotherms for CO_2, CH_4 and N_2 at 273 K and their corresponding single-site Langmuir-Freundlich curves (solid orange lines).